PHYSICAL REVIEW C VOLUME 36, NUMBER 6 DECEMBER 1987

Viewing the liquid-gas phase transition by measuring proton correlations

Scott Pratt
Department of Physics, University of Tennessee, Knoxville, Tennessee 37966

M. B. Tsang
National Superconducting Cyclotron Laboratory, Michigan State University, East Lansing, Michigan 48824
(Received 15 June 1987)

A formalism is developed for predicting two-particle correlations in terms of the final single-particle phase-space distributions which can be calculated from theoretical models. The ability to determine the phase-space distributions from experiment is discussed. It is shown that evaporation which characterizes the liquid phase and expansion which characterizes the gaseous phase have clear experimental signatures. An abrupt change in the behavior of the experimentally inferred lifetime is predicted near the threshold for the liquid-gas phase transition.

I. INTRODUCTION

Although modern heavy ion colliders easily reach the energy where the thermalized fireball is hot enough to leave the liquid phase of nuclear matter, there have been no unambiguous experimental signatures of the phase transition from single-particle spectra. If it were possible to view a motion picture of the collision for various beam energies it would be clear when the phase transition had taken place. A gas, by definition, will expand to fill the volume in which it is contained while a liquid will evaporate particles into the gaseous phase which then fills the volume. In a collision where the bombardment energy is below that needed to create a gas, the thermalized region will shrink and evaporate particles characterized by a decaying temperature. Whereas if the gaseous phase is initially created the thermalized region will expand due to the inner pressure, and if the system is hot enough it may even be described with hydrodynamics and result in collective expansion. This critical energy, corresponding to point "a" in the equation of state[1] in Fig. 1, labels the minimum density for which the pressure can be zero without being in the region of instability, $\partial P/\partial V \geq 0$. At slightly higher energies the system can not be at zero pressure and will expand and cool, perhaps passing through the mixed phase and fragmenting into gaseous and liquid components.[2]

Experimentally inferring the lifetime for the emission of particles for any given center of mass energy would give the essential features for distinguishing which picture of the collision is accurate. (Throughout this paper the collision is viewed in the center of mass frame and all momenta are described in that frame.) An evaporative emission is characterized by very long lifetimes, thousands of fm/c. The lifetimes are longest for the slowest particles, since the temperature falls very slowly once the source becomes cold.[3] A gas should expand and disperse in only a fraction of the time, perhaps less than 100 fm/c after maximum compression occurs.[4] Proton correlation measurements provide a viable method to extract these lifetimes.

Particles which are otherwise randomly emitted will interfere with each other due to final state interactions or exchange effects. The interference will be stronger for spatially smaller sources and is quantified through measuring the two-particle correlation function. The correlation function $C(\mathbf{p}_\alpha,\mathbf{p}_\beta)$ is the ratio of the probability of detecting two particles with momenta $\mathbf{p}_\alpha$ and $\mathbf{p}_\beta$ in the same event to the product of the probabilities of detecting them in different events. It is unity for random emission:

$$C(\mathbf{p}_\alpha,\mathbf{p}_\beta)=\frac{P(\mathbf{p}_\alpha,\mathbf{p}_\beta)}{P(\mathbf{p}_\alpha)P(\mathbf{p}_\beta)} \ . \tag{1}$$

In Sec. II we develop a formalism where the correlation function is uniquely determined by the final phase-space distribution of the collision $f(\mathbf{p},\mathbf{r})$. The spatial shape of $f(\mathbf{p},\mathbf{r})$ for a specific momentum $\mathbf{p}$ gives interesting information about the lifetime. For instance, a long lived source will stretch the final distribution $f(\mathbf{p},\mathbf{r})$ along the direction of $\mathbf{p}$. The phase-space distribution is readily extracted from a plethora of theoretical models: Boltzmann-Uehling-Uhlenbeck (BUU),[4] cascade,[5] thermodynamic,[6] fireball,[7] time dependent Hartree-Fock,[8] or evaporative. We show that measuring the correlation function for different values of the total momentum of the two-particle pair and for different directions of the relative momentum is vital when attempting to extract information about the lifetimes or collective motion from experiment.

The relevant features of this formalism are the following. (1) The correlation function is shown to depend on all the features of $f(\mathbf{p},\mathbf{r})$ but the lifetime is not uniquely determined. (2) Other correlations such as those caused by different impact parameters or rotational motion can be included. (3) The correlation function can be evaluated for two particles of different mass.

In Sec. III we present the essential features of $f(\mathbf{p},\mathbf{r})$ for several theoretical scenarios. These have quite different features which could be seen through correla-

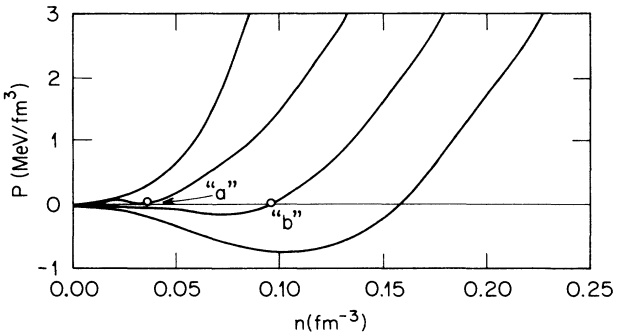

FIG. 1. The pressure is plotted against density for four isentropes taken from Ref. 1. Collisions with energies less than that of point "a" can find a stable value of the density such as point "b" at which to equilibrate with the vacuum and slowly evaporate nucleons. Collisions with a greater energy must continually expand since they must maintain a positive pressure.

tion measurements. Finally, we discuss the change in the behavior of the phase-space distributions near the threshold of the liquid-gas phase transition.

II. RESOLVING POWER OF THE CORRELATION FUNCTION

In the derivation of the correlation function we attempt to write the most general quantum mechanical state $|\eta\rangle$ and then calculate the probability $P(\mathbf{p}_\alpha,\mathbf{p}_\beta)$ of detecting two particles α and β with momenta $\mathbf{p}_\alpha$ and $\mathbf{p}_\beta$. For incoherent emission $P(\mathbf{p}_\alpha,\mathbf{p}_\beta)$ is then written in terms of the two-particle Wigner function $f(\mathbf{p}_\alpha,\mathbf{r}_\alpha;\mathbf{p}_\beta,\mathbf{r}_\beta)$. The two-particle function can be written as an average over impact parameters of the product of the one-particle functions; it therefore contains correlations due to varying impact parameters. For instance, detecting one particle biases towards those events with a higher multiplicity. There is also a correlation around the axis of rotation if a significant fraction of the energy is in rotational form.

The probabilities used in Eq. (1) to determine the correlation function can be written in terms of creation and destruction operators as

$$P(\mathbf{p}_\alpha,\mathbf{p}_\beta)=\sum_b \langle \eta_b \mid a_\alpha^\dagger(\mathbf{p}_\alpha)a_\beta^\dagger(\mathbf{p}_\beta)a_\beta(\mathbf{p}_\beta)a_\alpha(\mathbf{p}_\alpha)\mid \eta_b\rangle \ , \tag{2a}$$

$$P(\mathbf{p}_\alpha)=\sum_b \langle \eta_b \mid a_\alpha^\dagger(\mathbf{p}_\alpha)a_\alpha(\mathbf{p}_\alpha)\mid \eta_b\rangle \ . \tag{2b}$$

The sum over b represents the averaging over impact parameters. We attempt to write the most general N-body state $|\eta_b\rangle$ has a superposition of several wave packets described by $\eta_i(\mathbf{r},t)$,

$$|\eta_b\rangle=\left[\prod_i \int d^3r_\beta \eta_i(\mathbf{r}_\beta,t_i)\Psi^\dagger(\mathbf{r}_\beta,t_i)\right]|0\rangle \ . \tag{3}$$

We assume that the particles interact only pairwise after both particles have been created in their final state. This defines the formation of the final state. We picture the wave packets as being created when the reaction has diffused to the point that the particles no longer interact except with another particle with very similar momentum. When the relative momentum $\mathbf{p}_\alpha$-$\mathbf{p}_\beta$ is so large that several particles are commonly emitted within that range, we cannot predict the correlation function from simple two-body considerations. The relation between the creation operators at large times and those at times during which the particles are significantly interacting is

$$a_\beta(\mathbf{p}_\beta)a_\alpha(\mathbf{p}_\alpha)=\int d^3r_\alpha d^3r_\beta \Phi(\mathbf{p}_\alpha,\mathbf{p}_\beta;\mathbf{r}_\alpha,\mathbf{r}_\beta)\times\Psi(\mathbf{r}_\alpha,t)\Psi(\mathbf{r}_\beta,t) \ . \tag{4}$$

Here $\Phi(\mathbf{p}_\alpha,\mathbf{p}_\beta;\mathbf{r}_\alpha,\mathbf{r}_\beta)$ is the outgoing scattering wave function for particles with momentum $\mathbf{p}_\alpha$ and $\mathbf{p}_\beta$. Using Eqs. (3) and (4) one obtains an expression for the probabilities.

$$\begin{aligned}P(\mathbf{p}_\alpha,\mathbf{p}_\beta)&=\int d^3r'_\alpha d^3r'_\beta d^3r_\alpha d^3r_\beta \Phi^*(\mathbf{p}_\alpha,\mathbf{p}_\beta;\mathbf{r}'_\alpha,\mathbf{r}'_\beta)\Phi(\mathbf{p}_\alpha,\mathbf{p}_\beta;\mathbf{r}_\alpha,\mathbf{r}_\beta)\sum_{b,i,j}\eta_i^*(\mathbf{r}_\alpha,t_{ij}^>)\eta_j^*(\mathbf{r}_\beta,t_{ij}^>)\eta_j(\mathbf{r}_\beta,\mathbf{t}_{ij}^>)\eta_i(\mathbf{r}_\alpha,\mathbf{t}_{ij}^>)\\ &=\int d^3r'_\alpha d^3r'_\beta d^3r_\alpha d^3r_\beta \Phi^*(\mathbf{p}_\alpha,\mathbf{p}_\beta;\mathbf{r}'_\alpha,\mathbf{r}'_\beta)\Phi(\mathbf{p}_\alpha,\mathbf{p}_\beta;\mathbf{r}_\alpha,\mathbf{r}_\beta)\\ &\quad\times\int d^3p'_\alpha d^3p'_\beta \exp[-i\mathbf{p}'_\alpha\cdot(\mathbf{r}_\alpha-\mathbf{r}'_\alpha)-i\mathbf{p}'_\beta\cdot(\mathbf{r}_\beta-\mathbf{r}'_\beta)]\sum_{b,i,j} f_b\left[i,\mathbf{p}'_\alpha,\frac{(\mathbf{r}_\alpha+\mathbf{r}'_\alpha)}{2},t_{ij}^>\right]f_b\left[j,\mathbf{p}'_\beta,\frac{(\mathbf{r}_\beta+\mathbf{r}'_\beta)}{2},t_{ij}^>\right] \ .\end{aligned} \tag{5}$$

Here $t_{ij}^>$ is the latter of the two creation times, and the Wigner function $f_b(i,\mathbf{p}'_\alpha,\mathbf{r}_\alpha,t_{ij}^>)$ is defined as

$$f_b(i,\mathbf{p}_\alpha,\mathbf{r}_\alpha,t_{ij}^>)\equiv\int d^3x\, e^{i\mathbf{p}\cdot\mathbf{x}}\eta_i^*(\mathbf{r}_\alpha+\mathbf{x}/2,t_{ij}^>)\eta_i(\mathbf{r}_\alpha-\mathbf{x}/2,t_{ij}^>) \ . \tag{6}$$

The Wigner function represents the phase-space distribution of the emitted particles from a particle wave packet. If the total and relative momenta replace the individual momenta and the position of the center of mass and the relative coordinate replace the individual coordinates, the wave function can be factored into the relative wave function times the wave function of the center of mass. The two-particle probability can be expressed as

$$P(\mathbf{K},\mathbf{k})=\int d^3k'd^3r\, d^3\delta r\, d^3R\,\phi^*(\mathbf{k},\mathbf{r}+\delta\mathbf{r}/2)\phi(\mathbf{k},\mathbf{r}-\delta\mathbf{r}/2)\sum_{b,i,j} f_b(i,j,\mathbf{K},\mathbf{R},\mathbf{k}',\mathbf{r},t_{ij}^>)e^{-i\mathbf{k}'\cdot\delta\mathbf{r}} \ , \tag{7}$$

where $\mathbf{K}=\mathbf{p}_\alpha+\mathbf{p}_\beta$, $\mathbf{R}=(m_\alpha\mathbf{r}_\alpha+m_\beta\mathbf{r}_\beta)/(m_\alpha+m_\beta)$, $\mathbf{r}=\mathbf{r}_\alpha-\mathbf{r}_\beta$, and $\mathbf{k}=(m_\alpha\mathbf{p}_\beta-m_\beta\mathbf{p}_\alpha)/(m_\alpha+m_\beta)$. The relative wave function is ϕ and the two-particle Wigner function $f_b(i,j,\mathbf{K},\mathbf{R},\mathbf{k}',\mathbf{r},t_{ij}^{>})$ is the product of the single-particle Wigner functions.

This is the most general of formalisms, but there remains an arbitrariness as to the precise time at which particles are created. The exact form of $f_b(\mathbf{p},\mathbf{r})$ for individual wave packets is not determined by any standard theoretical model.

The formalism can be significantly simplified by making the semiclassical approximation that the dependence of $f_b(i,j,\mathbf{K},\mathbf{R},\mathbf{k}',\mathbf{r},t_{ij}^{>})$ on $\mathbf{k}'$ is slow. The dependence of $\phi^*\phi$ on $\delta\mathbf{r}$ is roughly proportional to $e^{i\mathbf{k}\cdot\delta\mathbf{r}}$ (and is independent of k for the exchange part of $\phi^*\phi$). If the two particle Wigner function $f_b(i,j,\mathbf{K},\mathbf{R},\mathbf{k}',\mathbf{r},t_{ij}^{>})$ does not depend strongly on $\mathbf{k}'$, then the integration over $\delta\mathbf{r}$ will allow $f(\mathbf{k}')$ to be approximated as $f(\mathbf{k})$ [or $f(\mathbf{k}=0)$ for the exchange part]. Furthermore, if the relative momentum $\mathbf{k}$ is small we consider $f(\mathbf{k}=0)$ only and Eq. (7) can be written as

$$P(\mathbf{K},\mathbf{k})=\int d^3r\,d^3R\;\phi^*(\mathbf{k},\mathbf{r})\phi(\mathbf{k},\mathbf{r}) \times\sum_{b,i,j} f_b(i,j,\mathbf{K},\mathbf{R},\mathbf{k}'=0,\mathbf{r},t_{ij}^{>}) \; . \tag{8}$$

The two-particle function $\int d^3Rf(k=0)$ is time independent since the relative momentum is zero. This allows the different Wigner functions to be evaluated at the same time which can be assumed to be infinite so that all particles would have been emitted. The indices i,j,b can then be suppressed to give

$$C(\mathbf{K},\mathbf{k})=\int d^3r\;\phi^*(\mathbf{k},\mathbf{r})\phi(\mathbf{k},\mathbf{r})F_K(\mathbf{r}) \; , \tag{9}$$

$$F_K(\mathbf{r})=\frac{\int d^3Rf(\mathbf{K},\mathbf{R},\mathbf{k}=0,\mathbf{r},t\to\infty)}{\int d^3r_\alpha d^3r_\beta f(\mathbf{p}_\alpha,\mathbf{r}_\alpha,t\to\infty)f(\mathbf{p}_\beta,\mathbf{r}_\beta,t\to\infty)} \; .$$

Equation (9) is identical to that of Koonin[9] except that the integration over time has been incorporated into $F_K(\mathbf{r})$. For a specific total momentum $\mathbf{K}$, the correlation function can only be measured for the three components of the relative momentum $\mathbf{k}$, and will only depend on the three dimensional probability for having two particles (with exactly the same velocity and with total momentum $\mathbf{K}$) separated by a distance $\mathbf{r}$.

The size and shape of $F_K(\mathbf{r})$ uniquely determines the correlation function for a particle pair with total momentum $\mathbf{K}$. It is independent of the position of the center of mass of the probability packet and is independent of the details of when the particles were created with respect to one another. An elongated source where the particles were created simultaneously or a long-lived compact one could in principle give rise to identical probability packets. However, a long-lived source will always yield an elongated distribution $F_K(\mathbf{r})$ (where the long dimension is always in the direction of $\mathbf{K}$) while a spatially stretched source might not always be stretched along the direction of the particles velocity. It is therefore preferable to measure the correlation function and thereby determine $F_K(\mathbf{r})$ for several different directions of $\mathbf{K}$ in order to confidently ascertain the lifetime.

Although $F_K(\mathbf{r})$ does uniquely determine the correlation function $C(\mathbf{K},\mathbf{k})$ there remains the question of whether $F_K(\mathbf{r})$ can be uniquely determined from measuring $C(\mathbf{K},\mathbf{k})$. Certainly, for noninteracting and nonidentical particles where $\phi^*(\mathbf{k},\mathbf{r})\phi(\mathbf{k},\mathbf{r})=1$, the function $F_K(\mathbf{r})$ cannot be determined. For identical but noninteracting particles, the exchange part of $\phi^*(\mathbf{k},\mathbf{r})\phi(\mathbf{k},\mathbf{r})$ which is $e^{2i\mathbf{k}\cdot\mathbf{r}}$ leads to a very complete determination of $F_K(\mathbf{r})$ from $C(\mathbf{K},\mathbf{k})$:

$$F_K(\mathbf{r})=\pm\int d^3k\;e^{2i\mathbf{k}\cdot\mathbf{r}}[C(\mathbf{K},\mathbf{k})-1] \; . \tag{10}$$

For nonidentical particles which interact through the Coulomb force there is a strong effect on the correlation function. However, for sources much smaller than the Bohr radius the correlation is independent of the size or shape of the source. The Bohr radius for protons is 58 fm, five to ten times larger than a typical nuclear source. Coulomb induced correlations therefore give little information about nuclear collisions.

The amount of information that can be extracted from correlations induced by short-range interactions from nonidentical particles depends very much on the details of the interaction and the phase-space distributions. Calculating Eq. (9) for various shapes of $F_K(\mathbf{r})$ is the best way of analyzing and resolving power of the correlation function. If the source size is much larger than the range of the potential, the only information that can be obtained is $F_K(\mathbf{r}=0)$ which can be considered as the inverse volume of the system, while details of the shape are not available.[10] The most attractive set of particles for correlation measurements are those whose correlations induced by Fermi-Dirac or Bose-Einstein statistics are not overly obscured by effects from the potential.

Proton-proton correlations are significantly influenced by all three of the above effects. In 1978 Koonin[9] calculated the correlation function for a Gaussian shaped source of size $R=3$ fm and a lifetime $v\tau=11.31$ fm. This yields the same correlation function as an instantaneous elongated source with a longitudinal size of 12 fm, along the direction of the total momentum, and a transverse size of 3 fm. The correlation functions in Fig. 2 are derived from the final phase-space distribution:

$$f(\mathbf{p},\mathbf{r})=\exp-[(x/3\text{ fm})^2+(y/3\text{ fm})^2+(z/12\text{ fm})^2] \; . \tag{11}$$

There is a significant difference in the correlation functions for different directions of the relative momentum, signifying that the elongation could be determined. The correlation appears much stronger when $\mathbf{k}$ is parallel to the long dimension of the source. When $\mathbf{k}$ is along the short dimension, the anticorrelation due to the Fermi nature of the protons more strongly cancels the positive correlation due to the attractive potential. A careful analysis must be performed to determine the amount of data necessary to measure these correlation functions with sufficient accuracy. The cut for different orientations of the relative momentum has been performed pre-

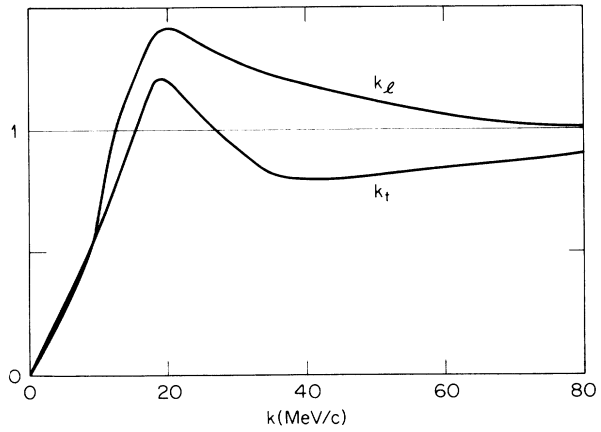

FIG. 2. The correlation function is shown for a Gaussian source where the transverse dimensions are 3 fm and the longitudinal dimension is 12 fm. The correlation is plotted for the relative momentum k being both parallel (k_l) and perpendicular (k_t) to the longitudinal direction. This demonstrates the resolution of correlation measurements for measuring the elongation of the final shape of the Wigner distributions.

viously for more energetic collisions, 1.8 GeV Ar on KCl. This is far above the threshold for creating a gas and no elongation was observed.[11]

III. PREDICTIONS FOR VARIOUS MODELS

In this section we discuss phase-space distributions calculated from three different theoretical models, an evaporative calculation,[12] a spherically symmetric exploding ball, and a BUU calculation.[4] The evaporative model should be realistic below the liquid-gas phase transition and the expanding ball might be realistic for highly energetic collisions. The BUU calculation is appropriate just above the phase transition. This comparison could point to interferometric signals of the critical temperature. From each model we extract the longitudinal (with respect to the particles momentum) and transverse size of $f(\mathbf{p},\mathbf{r})$ for several momenta. The dimensions $x(\mathbf{p})$,$y(\mathbf{p})$, and $z(\mathbf{p})$ are defined by

$$x(\mathbf{p})^2 \equiv \frac{\int d^3r\, d^3r'(\hat{\mathbf{x}}\cdot\mathbf{r}'-\hat{\mathbf{x}}\cdot\mathbf{r})^2 f(\mathbf{p},\mathbf{r}')f(\mathbf{p},\mathbf{r})}{\int d^3r\, d^3r' f(\mathbf{p},\mathbf{r})f(\mathbf{p},\mathbf{r}')} . \quad (12)$$

The variance of the phase-space distribution only contains a fraction of the information of the entire distribution, but the essential physical characteristics of elongation and overall volume are represented. This is a good meeting point for theory and experiment. It is probably unreasonable that any more information about the details of the shape of $f(\mathbf{p},\mathbf{r})$ could be extracted from experiment. When data is fitted to a particular form of $f(\mathbf{p},\mathbf{r})$, such as a Gaussian, the size as determined from fitting to Eq. (12) is probably independent of the particular form chosen. The essential physical information is contained in $x(\mathbf{p})$, $y(\mathbf{p})$, and $z(\mathbf{p})$.

The evaporative model is reasonable for temperatures where nuclear matter is in the liquid state. Particles are emitted independently according to their probability to escape the nuclear potential well. Since the source will cool and shrink while particles are evaporated, less energetic particles will more likely be emitted in the late stages when the source is cool. More energetic particles will escape early since they have a higher velocity, giving them more attempts to escape, and a greater energy to overcome barriers more easily. The temperature also falls very rapidly at the beginning of the reaction but very slowly later on. The most energetic particles escape within 50 fm/c while the less energetic ones are emitted over times that can be in the thousands of fm/c. The spread in the time $\tau=\langle(t-t')^2\rangle^{1/2}$ also falls rapidly with increasing energy. This leads to very elongated final phase-space distributions for these lower-energy particles where $v(E)\tau(E)$ is much larger than the size of the emitting region.

Figure 3 shows both the longitudinal and transverse spread as defined in Eq. (12) for protons emitted from an evaporative source where the initial temperature was 10 MeV and the initial charge was 30. We extracted the emission probabilities from a calculation that started at $T=18$ MeV, but we ignored emission from the early stages when $T>10$ MeV and the existence of a liquid phase is questionable. The spatial dimensions are plotted against the energy of the emitted protons. The evaporative model gives the emission probabilities and source sizes as a function of time. This is sufficient for calculating the final phase-space distributions. In addition to the longitudinal size x_L and the transverse size x_T, the average radial size $R=(x_T^2\cdot x_L)^{1/3}$ is also shown which corresponds to the total volume. The crucial signal for evaporative cooling is the strong elongation that rapidly diminishes for more energetic particles.

The opposite of the evaporative model is a simultaneous dissolution of a thermodynamically equilibrated

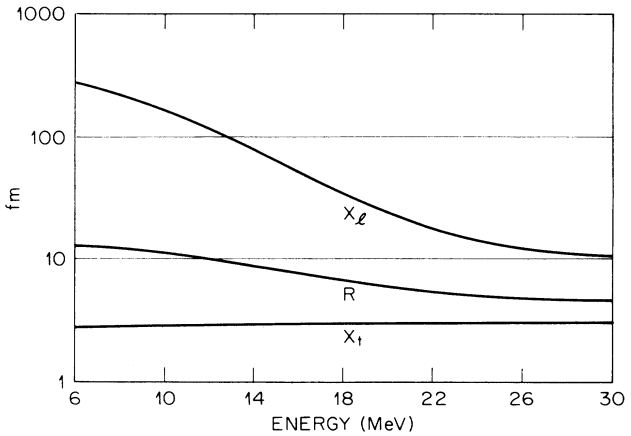

FIG. 3. Transverse and longitudinal sizes of the final Wigner distributions for specific momenta due to a spherically symmetric evaporative source ($T_0=10$ MeV) are shown as a function of energy. The momenta and corresponding energy are measured in the center of mass of the collision. Transverse and longitudinal refer to the direction of the specific momentum.

sphere with collective radial expansion increasing linearly from the center. The phase-space distribution for a particle with momentum p along the z axis is

$$f(\mathbf{p},\mathbf{r},\theta)=\exp\frac{(p^2-2mv_0pr\cos\theta/R+m^2v_0^2r^2/R^2)}{2mT}, \tag{13}$$

where R, T, and $v=v_0r/R$ refer to the radius, temperature, and local collective velocity. If there is no expansion velocity the source sizes are independent of energy. The scaling of the drop in source size with respect to the particle's energy depends only on the ratio of the collective momenta to the thermal energy (mv_0/T). We performed the calculation for $v_0/c=\frac{1}{3}$ and a temperature of 10 MeV, corresponding to two thirds of the energy in collective flow. The source sizes will fall more dramatically if the temperature is lowered or the collective velocity is raised. Both the longitudinal and transverse source sizes fall with energy as shown in Fig. 4. The difference between this scenario and that of the evaporative picture is the elongation. Evaporation can therefore only be distinguished from collective expansion after the correlation function has been measured for different directions of the relative momentum.

The BUU model considers particles to move and collide independently within a mean field which is generated by averaging hundreds of similar events together. The fermionic nature of the baryons is accounted for by limiting the phase-space density of the nucleons. Since fluctuations are neglected this model does not fare well near an instability such as where the pressure is zero at point "a" in Fig. 1. However, the model should do quite well above the threshold energy for such an instability. At these energies Pauli blocking is important and purely classical models are not appropriate.

A phase-space distribution was generated from a simulation of Ar on Ar at 60 MeV per nucleon. We choose to view this distribution for protons moving along the x axis, perpendicular to the beam. For each velocity we calculate the longitudinal size $x_L=\langle(x-x')^2\rangle^{1/2}$ and the transverse size $x_T=\langle(y-y')^2\rangle^{1/4}\langle(z-z')^2\rangle^{1/4}$ along with the radial size $R=x_L^{1/3}x_T^{2/3}$. The phase-space distributions for the BUU model were found by selecting the coordinates of the nucleons with the desired momentum. From these subsets the quantities x_L, x_T, and R were calculated and are shown in Fig. 5. Since there are a finite number of sample particles a nonzero width δp for the momentum gate must be chosen which causes the distribution to spread with time. Therefore the sizes are dependent on the time at which the phase-space coordinates are chosen. To minimize this spreading we picked a time just after the interactions had subsided, 300 fm/c after the initial contact.

For the faster particles ($p>200$ MeV/c) the fall in the longitudinal size with increasing energy suggests the source was rapidly cooling at the beginning of the reaction when the energetic particles were emitted. However, the less energetic particles could not have been emitted with zero momentum in the z direction after about 100 fm/c due to the transparency of the ions at this bombardment energy. Slower particles are therefore emitted with a common lifetime which leads to a rising source size with respect to energy, since the lifetime stretches the Wigner distribution proportional to $v(E)\cdot\tau(E)$. We expect that if one could measure the source size for values of p_z corresponding to the center of mass of the final target or beam fragments one might see further evidence of evaporation in the correlation function's behavior for low p_x particles. However, since

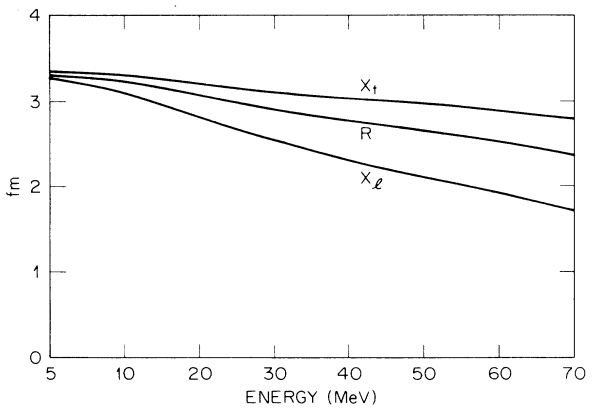

FIG. 4. Transverse and longitudinal sizes of the final Wigner distributions for specific momenta due to a spherically symmetric expanding source ($v/c=0.33r/R$, $R=4$ fm, $T=10$ MeV) are shown as a function of energy. The energy corresponds to this momentum as measured in the center of mass of the source. Transverse and longitudinal refer to the direction of the specific momentum.

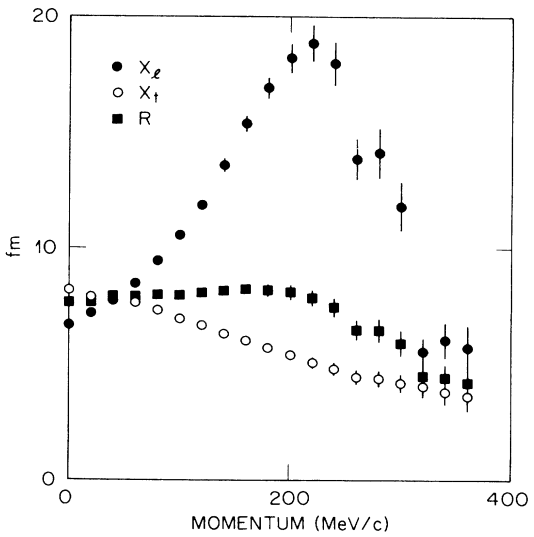

FIG. 5. Transverse and longitudinal sizes of the final Wigner distributions are plotted as a function of momenta which are perpendicular to the beam axis in the center of mass. These were calculated from a BUU code simulating a zero impact parameter Ar on Ar collision at 60 MeV/nucleon. Transverse and longitudinal refer to the direction of the momentum.

the fragments rapidity will vary greatly from event to event it would make such an experiment unreasonable. The transverse size also falls with energy due to the transparency.

Experiments have already been able to infer a source size as a function of the energy.[13–16] The source sizes extracted from 60 MeV/nucleon argon on gold collisions fall with increasing energy as shown in Table I. Both the expanding sphere model and the evaporative model exhibit this behavior despite the fact that they represent opposite extremes in viewing the collision. This emphasizes the necessity of inferring the elongation by measuring the correlation function for specific directions of the relative momentum.

TABLE I. Source sizes extracted from two-particle correlation measurements (Ref. 13) averaged over all directions of the relative momentum are shown for different energies in the center of mass of the collision (^{40}Ar + ^{197}Au; $E/A = 60$ MeV).

Pair	$E_1 + E_2$ (MeV)	R (fm)
p + p	25–75	6.0 (+0.5, −1.0)
	75–125	6.0±0.5
	125–175	5.5±0.4
	175–225	4.6±0.3
d + d	25–75	10.0±3.0
	75–125	7.0±2.0
	125–175	6.0±2.0
	175–225	5.0±1.0
	225–275	4.0±1.0
t + t	36–100	7.5±1.5
	100–180	6.0±1.5
	180–260	6.0±1.5
p + α	52–125	7.5 (+0.5, −1.0)
	125–200	6.7±0.4
	200–300	5.9±0.3
d + α	55–100	5.7±0.2
	100–200	4.8±0.2
	200–300	4.3±0.2
	300–400	4.4±0.2

IV. SUMMARY

We explained that a motion picture of the collision would certainly reveal whether the initial thermalized fireball was in the liquid or the gas phase by whether the constituents were evaporated individually or collectively after an expansion of the thermalized region. In Sec. II we demonstrated that the correlation functions depends only on the final phase space distribution, providing a snapshot of the end of the reaction. This contains the necessary physical information. The nucleons of a given velocity from an evaporative source will be stretched out along the direction of that velocity due to the long lifetime of a cooling and shrinking emitter. Figure 2 demonstrates that the elongation can be determined from correlation measurements. But, to see this shape, experiments must be able to measure the correlation functions $C(\mathbf{K},\mathbf{k})$ for a variety of directions of the relative momentum $\mathbf{k}$. The other necessary signal for an evaporative source is the fall in longitudinal size with respect to increasing momentum $\mathbf{K}/2$ of the emitted particles. Elongation signals a long lived source. Decreasing elongation with increasing momentum signals a cooling one. This requires greater statistics than what has been available from previous experiments, but we believe that the information is worth the effort.

The gaseous phase is not so clearly signaled. BUU calculations above the energetic threshold for creating a gas yield fundamentally different predictions for the final phase-space distributions and therefore the interferometry. We should also emphasize that even if another theoretical scenario is appropriate for describing the collision, the unique predictions for the correlation functions will stringently test the theory.

ACKNOWLEDGMENTS

Enlightening discussions with P. Siemens were greatly appreciated. This work was supported by the National Science Foundation under Grants PHY-8608418 and PHY-8312245.

[1]B. Friedman and V. R. Pandharipande, Nucl. Phys. **A361**, 502 (1986).
[2]J. Lopez and P. J. Siemens, Nucl. Phys. **A431**, 728 (1984).
[3]D. H. Boal and H. DeGuise, Phys. Rev. Lett. **57**, 2901 (1986).
[4]J. Aichelin and G. Bertsch, Phys. Rev. C **31**, 1730 (1985); J. Aichelin, *ibid.* **33**, 537 (1986).
[5]G. Bertsch and J. Cugnon, Phys. Rev. C **24**, 2514 (1981).
[6]A. Mekjian, Phys. Rev. Lett. **38**, 540 (1977)..
[7]G. D. Westphal *et al.*, Phys. Rev. Lett. **37**, 1202 (1976).
[8]S. E. Koonin, Prog. Part. Nucl. Phys. **4**, 283 (1980).
[9]S. E. Koonin, Phys. Lett. **70B**, 43 (1977).
[10]B. K. Jennings, D. H. Boal, and J. C. Shillcock, Phys. Rev. C **33**, 1303 (1986).
[11]F. Zarbakhsh *et al.*, Phys. Rev. Lett. **46**, 1268 (1981).
[12]W. A. Friedman and W. G. Lynch, Phys. Rev. C **28**, 16 (1983); **28**, 950 (1983).
[13]J. Pochodzalla *et al.*, Phys. Lett. B **174**, 36 (1986); J. Pochodzalla *et al.*, Phys. Rev. C **35**, 1695 (1986).
[14]C. B. Chitwood *et al.*, Phys. Lett. B **172**, 27 (1986).
[15]W. G. Lynch *et al.*, Phys. Lett. **168B**, 274 (1982); W. G. Lynch *et al.*, Phys. Rev. Lett. **51**, 1850 (1983).
[16]P. Kristiansson *et al.*, Phys. Lett. **155B**, 31 (1985).